Ionization effects on spectral signatures of quantum-path interference in high-harmonic generation

M. Holler[1,*], A. Zaïr[1], F. Schapper[1], T. Auguste[2], E. Cormier[4], A. Wyatt[3], A. Monmayrant[3], I. A. Walmsley[3], L. Gallmann[1], P. Salières[2], and U. Keller[1]

[1] *Physics Department, ETH Zurich, CH-8093 Zurich, Switzerland*
[2] *CEA-Saclay, IRAMIS, Service des Photons, Atomes et Molécules, 91191 Gif-sur-Yvette, France*
[3] *Clarendon Laboratory, University of Oxford, Parks Road, Oxford OX1 3PU, UK*
[4] *CELIA, Université Bordeaux I, CEA, CNRS, UMR 5107, 33405 Talence cedex*
[*] *Corresponding author: holler@phys.ethz.ch*

Abstract: The interference between the emission originating from the short and long electron quantum paths is intrinsic to the high harmonic generation process. We investigate the universal properties of these quantum-path interferences in various generation media and discuss how ionization effects influence the observed interference structures. Our comparison of quantum-path interferences observed in xenon, argon, and neon demonstrates that our experimental tools are generally applicable and should also allow investigating more complex systems such as molecules or clusters.

OCIS codes: (270.1670) Coherent optical effects; (270.6620) Strong-field processes.

References and links

1. P. B. Corkum, "Plasma perspective on strong-field multiphoton ionization," Phys. Rev. Lett. **71**, 1994-1997 (1993)
2. K. J. Schafer, B. Yang, L. DiMauro, and K. C. Kulander, "Above threshold ionization beyond the high harmonic cutoff," Phys. Rev. Lett. **70,** 1599-1602 (1993).
3. A. Zaïr, M. Holler, A. Guandalini, F. Schapper, J. Biegert, L. Gallmann, U. Keller, A. S. Wyatt, A. Monmayrant, I. A. Walmsley, E. Cormier, T. Auguste, J. P. Caumes, and P. Salières, "Quantum path interferences in high-order harmonic generation," Phys. Rev. Lett. **100**, 143902 (2008).
4. M. Lewenstein, P. Salières, and A. L'Huillier, "Phase of the atomic polarization in high-order harmonic generation," Phys. Rev. A **52**, 4747-4754 (1995).
5. P. Salières, B. Carré, L. Le Déroff, F. Grasbon, G. G. Paulus, H. Walther, R. Kopold, W. Becker, D. B. Milosevic, A. Sanpera, and M. Lewenstein, "Feynman's path-integral approach for intense laser-atom interactions," Science **292**, 902-905 (2001)
6. P. Salières, A. L'Huillier, and M. Lewenstein, "Coherence control of high-order harmonics," Phys. Rev. Lett. **74**, 3776-3779 (1995)
7. Z. Chang, A. Rundquist, H. Wang, I. Christov, H. C. Kapteyn, and M. M. Murnane, "Temporal phase control of soft-x-ray harmonic emission," Phys. Rev. A **58**, R30-R33 (1998)
8. M. B. Gaarde, F. Salin, E. Constant, Ph. Balcou, K. J. Schafer, K. C. Kulander, and A. L'Huillier, "Spatiotemporal separation of high harmonic radiation into two quantum path components," Phys. Rev. A **59**, 1367-1373 (1999)
9. P. Salières, A. L'Huillier, P. Antoine, and M. Lewenstein, "Study of the spatial and temporal coherence of high-order harmonics," Adv. At. Mol. Opt. Phys. **41**, 83-142 (1999)
10. C. Lyngå, M. B. Gaarde, C. Delfin, M. Bellini, T. W. Hänsch, A. L' Huillier, and C.-G. Wahlström, "Temporal coherence of high-order harmonics," Phys. Rev. A **60**, 4823-4830 (1999)
11. W. Boutu, S. Haessler, H. Merdji, P. Breger, G. Waters, M. Stankiewicz, L. J. Frasinski, R. Taieb, J. Caillat, A. Maquet, P. Monchicourt, B. Carre, and P. Salières, "Coherent control of attosecond emission from aligned molecules," Nature Phys. **4**, 545-549 (2008)
12. S. Baker, J. S. Robinson, C. A. Haworth, H. Teng, R. A. Smith, C. C. Chirila, M. Lein, J. W. G. Tisch, and J. P. Marangos, "Probing Proton Dynamics in Molecules on an Attosecond Time Scale," Science **312**, 424-427 (2006)

#107743 - $15.00 USD Received 20 Feb 2009; revised 20 Mar 2009; accepted 20 Mar 2009; published 25 Mar 2009

1. Introduction

The interaction of an intense linearly polarized laser field with an atom leads to the generation of high-order harmonics. The high harmonic generation (HHG) process can be understood by means of a semiclassical three-step model: In a first step the atomic potential barrier is lowered by the strong laser field allowing for tunnel ionization; in a second step the free electron quivers in the electric field of the laser. For some release times, the electron is driven back to the parent ion and, in a third step, recombines to the ground state emitting a XUV photon. This process repeats itself every half cycle of the generating pulse, thus the XUV spectrum consists of odd harmonics of the fundamental frequency [1, 2]. Depending on the spectral range, several different electron trajectories can lead to recombination and contribute to the harmonic emission. Electron wave-packets following different trajectories leading to the same emitted photon energy usually acquire a different phase. The resulting phase difference between the various contributions is expected to reveal itself through interference effects. Quantum mechanical models confirm the conclusions drawn based on the semiclassical model. Although interference effects have been predicted long ago, they have been observed only recently for HHG in argon [3]. Here, we show that these quantum path interferences (QPI) are indeed an intrinsic phenomenon of HHG and can be observed for various generation media. We discuss results obtained in xenon, argon and neon and investigate how the different ionization potential of these gases affects the signature of QPI, both experimentally and theoretically.

2. Theoretical background

The emission of plateau harmonics (labeled by their order q) is dominated by the contribution of the two shortest electron trajectories. The so-called 'short' trajectory ($j=1$) is characterized by a short electron excursion time $\tau_q^{(1)} < 0.65\,T$, where T is the laser period. The 'long' trajectory ($j=2$) has a longer excursion time $0.65T < \tau_q^{(2)} < T$. In the cutoff region, these trajectories merge into a single one. The action accumulated by the electron wave-packet along the trajectories determines the phase of the corresponding harmonic contributions. The harmonic phase can thus be approximated by the product of the ponderomotive energy U_p with the electron excursion times $\tau_q^{(j)}$. This results in an intensity dependence of the harmonic phase [4, 5]:

$$\phi_q^{(j)}(r,t) \approx -U_p \tau_q^{(j)} \approx -\alpha_q^{(j)}(I(r,t)) \cdot I(r,t),$$

where $I(r,t)$ is the laser intensity and $\alpha_q^{(j)}$ is roughly proportional to the electron excursion time.

The harmonic yield of plateau harmonics can exhibit strong modulations with respect to the laser intensity if both trajectories contribute to a comparable extent as a result of their interference. However, in most practical experimental configurations, the spatial and temporal dependence of the harmonic phase smears out the interferences in the macroscopic response. In order to enable their experimental observation, special measures have to be taken in the design of the experiment. This is the reason why these interferences have not been observed experimentally until the work reported in Ref. [3].

To overcome temporal smearing, we exploit the intrinsic properties of the harmonic chirp, related to the harmonic phase through

$$\Delta\omega^{(j)}(t) = -\frac{\partial \phi_q^{(j)}(t)}{\partial t} = \frac{\partial \alpha_q^{(j)}(I(t))}{\partial I}\frac{\partial I(t)}{\partial t} \cdot I(t) + \alpha_q^{(j)}(I(t)) \cdot \frac{\partial I(t)}{\partial t} \approx \alpha_q^{(j)} \cdot \frac{\partial I(t)}{\partial t},$$

where $\Delta\omega = \omega - \omega_q$ [6, 7, 8, 9]. The harmonic chirp spectrally shifts the harmonic emission generated on the leading edge to higher frequencies and the emission of the trailing edge to

#107743 - $15.00 USD Received 20 Feb 2009; revised 20 Mar 2009; accepted 20 Mar 2009; published 25 Mar 2009

lower frequencies. By limiting the observation of the interferences to the exact harmonic frequency ω_q we avoid temporal averaging. This results from the fact that the harmonic chirp ensures that the generation of this center frequency is always confined to the instant of maximum laser peak intensity in a Gaussian or similarly bell-shaped pulse.

Spatial effects blurring the interference fringes need also to be suppressed in order to observe QPI. We circumvent longitudinal averaging (along the propagation direction) by choosing a generation medium shorter than the Rayleigh range of the laser. The additional transverse spatial averaging can be avoided by performing a far-field spatial filtering of the harmonic emission. Indeed, the transverse variation of the laser intensity results in a different phase front curvature of the short and long path contributions [6, 8, 9, 10], leading to interference rings in the far-field pattern. Applying a far-field spatial filter thus limits the averaging effect that would smear out QPI.

Under such conditions of spectral and spatial filtering, QPI can be detected by varying the generating laser intensity. In the experiments reported here, we put the main emphasis on investigating how QPI scale to different generation media and what role ionization effects play for the observed interference structures. Ionization effects affect the single-atom response of the medium via ground-state depletion and the macroscopic harmonic emission via free electron dispersion and phase matching.

3. Results and discussion

In the following, we present both experimental and theoretical results obtained in different rare gases. The generation conditions are the same as those described in Ref. [3]. Laser pulses with a center wavelength of 800 nm and a duration of 30 fs are sent through an iris aperture and focused by a spherical mirror into a pulsed gas jet. The ROC of the focusing mirror was 50 cm for the case of argon and xenon, and 25 cm for the case of neon. A half-wave plate and a polarizer control finely the energy of the laser pulses. The jet is movable along the propagation direction to control phase matching conditions. The emitted harmonic radiation is refocused by a spherical gold mirror (ROC = 30 m) in grazing incidence. This mirror is movable perpendicular to the propagation direction for lateral windowing of the beam. The refocused harmonics pass an aluminum filter (150 nm thickness) and hit the entrance slit of an XUV spectrometer consisting of a reflective grating and a XUV CCD.

We simulate the full macroscopic response measured in the experiments using the strong-field approximation (SFA) dipole and a three-dimensional propagation code that solves the propagation equations for the laser and harmonic fields in the paraxial and adiabatic approximations.

A generic behavior with respect to the phase matching conditions, independent of the ionization potential of the generating medium, is observed. When selecting the short trajectory (jet after the laser focus), we observe spectrally narrow harmonics as a result of the small frequency chirp of the short trajectory. Their amplitude increases monotonically with the laser intensity since in this case only one trajectory is detected. With the experimental setup described above, we can filter out transverse sections of the emitted beam in its far field distribution. Changing the far field spatial selection from on-axis to off-axis with phase matching optimized for the short trajectory only affects the overall detected harmonic yield, reducing it by roughly one order of magnitude.

In contrast to the previous situation, both trajectories are phase-matched for a jet placed before the laser focus. For an on-axis spatial selection in the far field, the harmonic signal is still spectrally narrow because stronger on-axis emission from the short trajectory with its lower divergence is detected. When selecting the off-axis portions of the beam, a clear broadening of the plateau harmonic spectral width with increasing laser intensity is observed. This is the typical signature of the long trajectory resulting from its larger intrinsic chirp. When properly balancing the relative contributions from the short and the long trajectories by adjusting the position of the far-field spatial filter, interference contrast is maximized and a clear modulation of the harmonic yield with laser intensity occurs. This interpretation is

#107743 - $15.00 USD Received 20 Feb 2009; revised 20 Mar 2009; accepted 20 Mar 2009; published 25 Mar 2009

further supported by the fact that in the cutoff region we neither observe significant broadening nor any modulations since only one quantum path exists.

The harmonic spectra measured in argon in the optimized conditions for QPI observation are shown in Fig. 1. The intensity for barrier suppression in argon (ionization potential 15.8 eV) is $2.5 \cdot 10^{14}$ W/cm^2. Below this intensity, we observe several modulation periods corresponding to QPI. For higher intensities, the onset of ionization effects results in both an asymmetric shape of the different harmonic orders and a much weaker modulation of the on-axis harmonic signal. These trends are reproduced in our simulations, in particular for harmonic 21 shown in Fig 1b (6 mrad wide far-field integration window centered 17 mrad off axis). The experimentally measured average modulation periodicity $\sim 3 \cdot 10^{13}$ W/cm^2 is consistent with our simulations indicating that the modulations are caused by first order QPI [3].

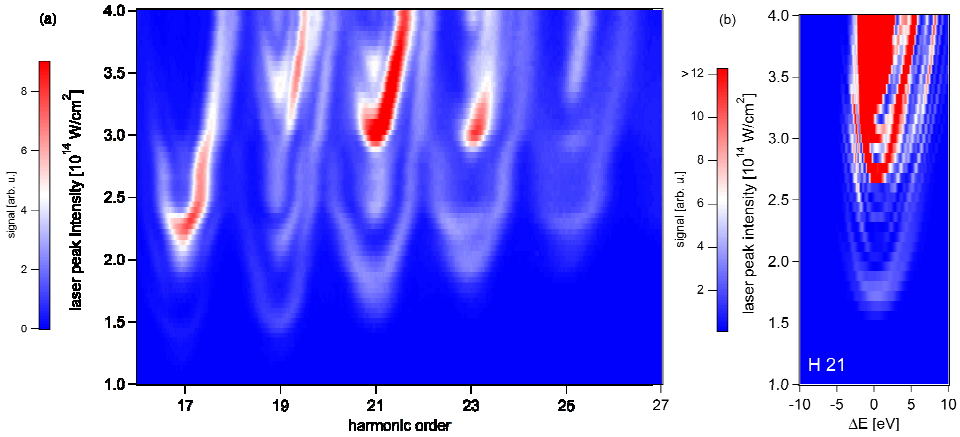

Fig. 1. Harmonic spectra generated in argon versus laser peak intensity with short and long trajectory phase-matched and off axis spatial selection: (a) measured spectra, (b) simulated spectra around harmonic 21.

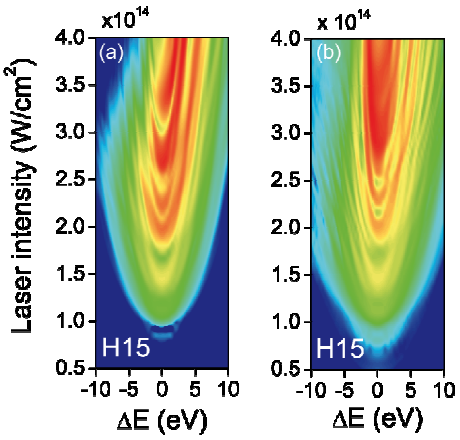

Fig. 2. QPI dependence on pressure calculated for H15. (a) P = 1 Torr. (b) P = 10 Torr. The harmonic intensity is plotted with a logarithmic scale normalized for each plot to the maximum signal.

Different particle densities in the interaction region do not affect the described spectral behavior significantly in our measurements as well as in our simulations. Especially the modulation periodicity remains unchanged, indicating that dispersion does not play a dominant role for the harmonic yield modulations. However, closer inspection reveals subtle changes in the fine structure of the fringes when the pressure is increased. This is illustrated

#107743 - $15.00 USD Received 20 Feb 2009; revised 20 Mar 2009; accepted 20 Mar 2009; published 25 Mar 2009

in Fig. 2 showing simulations for harmonic 15 of argon for gas pressures of 1 and 10 Torr. While the modulations at the harmonic central frequency are rather robust, the fine details within the fringe structure are pressure dependent in particular on the blue side and at high intensities. An apparent splitting of the fringes can be observed at 10 Torr for intensities between $2.5 \cdot 10^{14}$ W/cm^2 and $3 \cdot 10^{14}$ W/cm^2. Since this splitting appears only for the high-pressure scenario and above the barrier suppression intensity, it can clearly be attributed to macroscopic nonlinear optical effects.

We further analyzed the origin of the different fringe structures with detailed simulations. Figure 3 shows the result of the full model compared to simulations with either all ionization effects switched off or only the single-atom level ionization effects included. The latter case thus includes the medium depletion but does not take into account the macroscopic effects of free-electron dispersion. The simulations show that the asymmetry of the harmonic spectrum at high intensity results from ground state depletion, which is a single atom effect. The harmonic signal on the red side of the spectrum is reduced because on the trailing edge of the generating laser pulse the medium is already depleted. The asymmetry of the harmonic spectrum is thus a direct result of the time-to-frequency mapping caused by the harmonic chirp. The simulated data in Fig. 3 also reveal that the apparent fringe splitting on the blue side of the harmonic line and other distortions of the fringe structure are a direct consequence of free-electron dispersion. These free electrons are created on the leading edge of the pulse for intensities beyond barrier suppression. Since the free electrons are concentrated on the beam axis, it is expected that they affect the emission from the short trajectory more strongly than from the long trajectory due to their different phase-matching properties [5,8]. Interference in the far field between contributions from the short and long trajectory originating from different transverse locations in the medium explains the observed distortions in their relative phase.

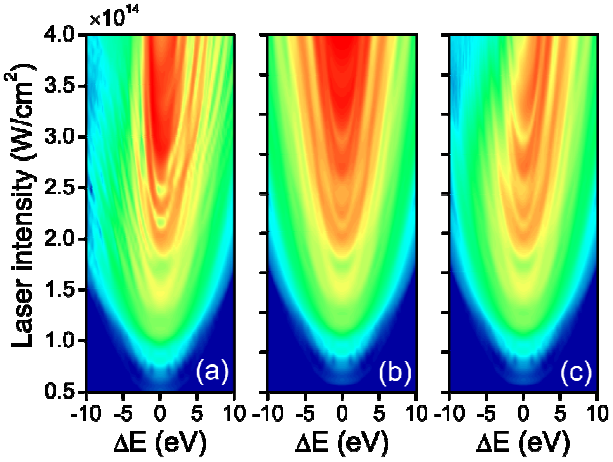

Fig. 3. Simulated QPI for H15 in argon at a pressure of 10 Torr. (a) full simulation, (b) ionization switched off, (c) with depletion, but free electron dispersion switched off.

Xenon with its lower ionization potential of 12.1 eV shows saturation effects at lower intensities than in argon. The intensity for barrier suppression is $I_{BS} = 8.7 \cdot 10^{13}$ W/cm^2. Above this intensity, the harmonic yield saturates and the effective driver pulse duration contributing to the harmonic emission gets shorter with increasing laser intensity due to the fast medium ionization. Only the leading part of the pulse generates harmonics, resulting in a strong asymmetry of the harmonic spectra. Meanwhile, the harmonic chirp increases further, which leads to asymmetric broadening on the blue side only (Fig. 4).

#107743 - $15.00 USD Received 20 Feb 2009; revised 20 Mar 2009; accepted 20 Mar 2009; published 25 Mar 2009

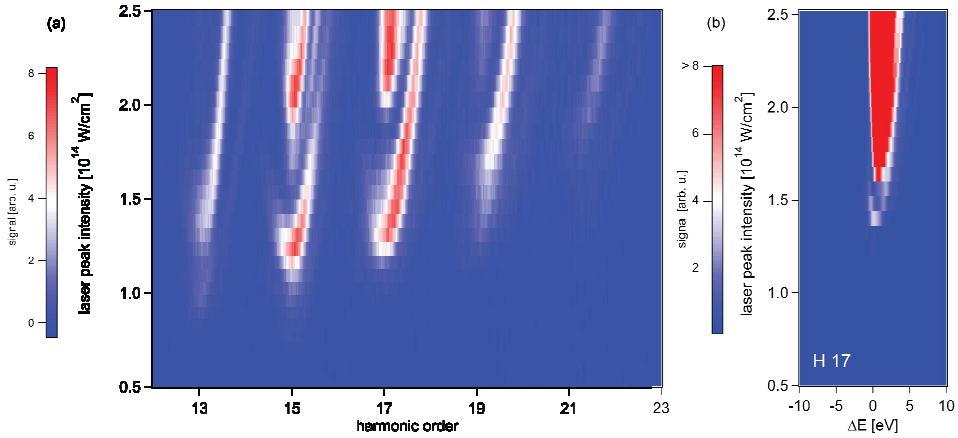

Fig. 4. (a) Measured harmonic spectra generated in xenon versus laser peak intensity, (b) simulated spectrum for harmonic order 17.

In the case of neon, the high ionization potential of 21.6 eV leads to a saturation intensity, which is approximately one order of magnitude higher than in the case of xenon. Therefore it is possible to generate efficiently high harmonics well below the saturation intensity, opening the way to study the QPI over a wide range of intensities without being limited by ionization. As expected, the data displayed in Fig. 5 shows no sign of blue shift. Within the range of covered intensities, we are able to clearly identify about five modulation periods of the harmonic yield with an average periodicity of $\sim 8 \cdot 10^{13}$ W/cm^2.

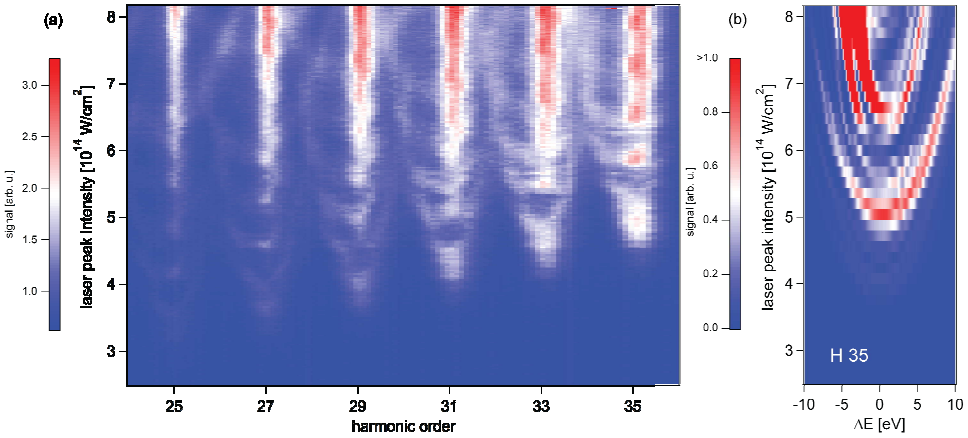

Fig. 5. (a) Experimental harmonic spectra generated in neon with respect to the laser peak intensity: over the full range of accessible intensities located below ionization threshold neither a blue shift nor a saturation of harmonic signal at the harmonic central frequency is observed, (b) simulated spectrum for harmonic order 35.

4. Conclusion

The presented data show that experimental and theoretical conditions can be found allowing for the observation of quantum path interferences in high-harmonic generation independent of the harmonic generating medium. This is made possible through proper spectral and spatial filtering. The filtering prevents spatial and temporal variations of the interference conditions from smearing out the fringes. We discussed the influence of the generation medium, and more specifically ionization effects, on the observed interference structures. The comparison of measurements taken in different gases allowed us to study the behavior of QPI with laser intensities above, around and below the ionization threshold. Depending on this regime, the

#107743 - $15.00 USD Received 20 Feb 2009; revised 20 Mar 2009; accepted 20 Mar 2009; published 25 Mar 2009

plateau harmonics exhibit intensity-dependent features such as saturation of the harmonic yield, spectral blue shift, and trajectory dependent spectral broadening. The measurements are well supported through simulations. Our method provides the possibility of investigating this behavior in more complex systems such as molecules or clusters. Recent experiments have shown that in small molecules, such as CO_2, N_2, H_2, D_2, the continuum dynamics of the electron wavepacket (which is at the origin of QPI) is similar to that of atoms, at least for the short trajectories [11, 12]. One can thus expect that QPI will be observable in these systems and that its interferometric sensitivity will reveal differences between the molecular and the atomic continua. Our method is a general, robust tool to collect information directly in the spectral domain of the harmonic generation process including its temporal dynamics under varying experimental conditions.

Acknowledgments

This research was supported by the NCCR Quantum Photonics (NCCR QP), research instrument of the Swiss National Science Foundation (SNSF), the French Agence Nationale de la Recherche (ANR-05-BLAN-0295-01, ATTO-SCIENCE), COST-STSM-P14-01910, and the European Commission through the RTN XTRA (MRTN-CT-2003-505138).

#107743 - $15.00 USD Received 20 Feb 2009; revised 20 Mar 2009; accepted 20 Mar 2009; published 25 Mar 2009